Symmetric assembly and disassembly of an ecological network

Jason M. Tylianakis[1,2], Laura B. Martínez-García[3,4], Sarah J. Richardson[3], Duane A. Peltzer[3], Ian A. Dickie[3,5]

[1] Centre for Integrative Ecology, School of Biological Sciences, University of Canterbury, Private Bag 4800, Christchurch 8140, New Zealand.

[2] Department of Life Sciences, Imperial College London, Silwood Park Campus, Buckhurst Road, Ascot, Berkshire SL5 7PY, United Kingdom

[3] Landcare Research, PO Box 69040, Lincoln 7640, New Zealand

[4] Department of Soil Quality, Wageningen University. P.O. Box 47. Wageningen 6700 AA , The Netherlands

[5] Bio-protection Research Centre, Lincoln University, PO Box 85084, Lincoln 7647, New Zealand

Abstract

The position of species in interaction networks can predict their extinction probability. However, the processes whereby these network roles emerge and persist, then decay during ecosystem development are unknown. Here we study networks of plant and arbuscular mycorrhizal fungal (AMF) communities along a 120,000 yr soil chronosequence, with two distinct phases: progressive (i.e. assembly, where plant richness and biomass increase) and retrogressive (i.e. disassembly, where plant richness and biomass decline with declining nutrients). We find that the order of interaction formation during progression mirrors that of interaction extinction during retrogression, and that interactions in sites moving forwards or backwards from the (12,000 yr) site of peak biomass were nested subsets of the interactions at that site. Network assembly and disassembly were symmetrical, self-reinforcing processes that together generated key attributes of network architecture. Plant species that had high AMF-partner overlap with others in the community (measured as ‘closeness centrality') were best able to attract and retain new AMF partners, and AMF species with high partner overlap were better able to retain their interactions with plants. In contrast, interaction generalism (‘node degree’) per se was a poor predictor of partner attraction during assembly or retention during

disassembly. These results could be used to predict extinction sequences based on community assembly or network roles, identify focal points for invasions, and suggest trajectories for ecosystem restoration.

Keywords: community assembly, succession, ecosystem development, retrogression, mutualist network, mycorrhizal symbiosis, preferential attachment

Introduction

The arrangement of species interactions in ecological networks can be critical for the stability and functioning of ecosystems (1-3). However the processes that generate and maintain network structure during ecosystem development are unresolved. The generally accepted hypothesis for complex network assembly is that new nodes (e.g., species) preferentially connect with those that are linked to many immediate neighbors (4) (i.e. generalist nodes of high 'degree'). This 'preferential attachment' was predicted (5), then shown empirically (6), to occur during the assembly of pollination networks within a season. In contrast, a study of long-term changes to pollination networks found that less-connected species preferentially attracted new interactions (7), such that the importance of preferential attachment based on node degree remains unclear for ecological networks. Although studies on the generation of network architecture have largely focused on node attachment during network assembly, the opposing process of preferential detachment can theoretically produce the same architecture as preferential attachment (8, 9). This possibility is strengthened by empirical findings that pollination networks show preferential loss of less-connected species and their interactions (7, 10). Finally, it is possible that network architecture may be generated by preferential attachment during community assembly, and maintained by preferential detachment during disassembly. This would imply that the same rules may operate during both the assembly and disassembly of ecological networks (11), but this hypothesis remains untested.

Here we study interaction network assembly and disassembly in a community of plants and arbuscular mycorrhizal fungi (AMF)(12) throughout 120,000 years of ecosystem development. Arbuscular mycorrhizal fungi are essential mutualists of most terrestrial plants (13), and have typical within-site diversity comparable to plant communities (14). Moreover, the high importance of species interactions for determining AMF community composition (15, 16) demands a focus on interactions (17) for these systems, within the context of soil nutrients which can also be important drivers of community structure (18). First, we test whether network assembly and disassembly processes are random or related to species' position in the network. Second, we test the hypothesis (11) that attachment and detachment are symmetrical, such that the process and order of disassembly mirror those during assembly. Finally, we use simulations to determine how non-random assembly and disassembly processes impact upon key aspects of network architecture.

The first requirement for an interaction to take place is an encounter, and if co-occurrence rates between AMF propagules and plants were merely stochastic (19), we would expect newly-arriving species to interact preferentially with the most abundant species in the site. An established AMF species that has used its associations with many plant species to develop an extensive mycelium network could also be a beneficial partner, due to a reduction in initial construction costs and immediate access to a large soil volume (20, 21). In this sense, the local abundance of a species, along with the number of species with which it interacts, may partly indicate its quality as a mutualist. If plants or AMF exhibit selectivity in their interaction partners (22), we might therefore expect a general pattern of newly-arriving species having a greater probability of interacting with generalist species, i.e. traditional preferential attachment based on species degree (4, 6). This pattern could also occur simply if generalists are least selective in the partners they accept. Moreover, high AMF diversity can reduce competition among plant species and provide insurance against variability in soil conditions, such that plant species that interact with many AMF experience increased biomass (23). This greater biomass could make AMF-generalist plants more attractive partners because they have the capacity to provide more carbon across a wider range of conditions.

However, the benefits of interacting with generalists may depend in part on whether they share their interaction partners with other species. Although AMF typically interact with many plant species, there is growing evidence that their composition (15) and fitness can differ across plant hosts (24). Host-plant selectivity may not necessarily be species specific, but rather groups of AMF can associate with ecological groups of plants (25). Closely-related AMF also tend to co-occur in a given location (26), and closely-related organisms tend to share interaction partners (27). We may therefore expect large interacting consortia of ecologically-similar, and in some cases phylogenetically related, plants and fungi to form at a given successional stage, with the dominant consortium potentially differing between early-successional generalist species and later-successional forest species (14, 25). Thus, at each stage of ecosystem development, newly-arriving fungi may have a higher probability of interacting with plants in the dominant ecological group at that stage, which will already interact with species from the dominant fungal group. These plant species would not only (or even necessarily) be the most generalist individually, but they would have high AMF-partner overlap with other plant species in the dominant group at that stage (i.e. with the majority of species in the site). Species that have high interaction-partner overlap with others in the network may also receive fitness benefits from positive indirect effects (1), making them more reliable interaction partners. We therefore hypothesise that the attractiveness of a species to new arrivals may depend on its sharing of interaction partners with other species (see Fig. S1 for our approach to measuring partner overlap).

To test these hypotheses, we used a dataset (15) on plant-AMF networks that were sampled at different sites along a long-term (>120 kyr) chronosequence comprising all stages of ecosystem development, including retrogression (28). Chronosequences represent a powerful tool for understanding long-term co-ordinated changes amongst species and their interactions, resource availability and ecosystem processes (28). Strong gradients from initial N-limitation to eventual strong P-limitation of ecosystem processes drive turnover of plant and AMF species (15, 29). We treated ecosystem progression (during which plant species richness and biomass

129 increase (29)) as the assembly phase, and ecosystem retrogression (during which
130 strong P-limitation causes a loss of plant diversity and biomass (29)) as the network
131 disassembly phase. We defined attachment as the first ecosystem stage at which a
132 plant or AMF species was observed along the chronosequence, and detachment as
133 the final ecosystem stage in which a species was observed.
134
135 **Results**
136 In total our samples yielded 33 operational taxonomic units (OTUs, hereafter
137 referred to as species) of AMF and 53 species of plant, among which we observed
138 399 pairwise interactions (i.e. links, defined as the colonisation of a plant root by an
139 AMF species) (Fig. 1). There were an average of 16 AMF (SD = 3.33) and 10.8 (SD =
140 3.77) plant species, with 137.5 (SD = 24.14) interactions per site (Table S1). The AMF
141 community changes and turnover along the chronosequence have been described in
142 detail elsewhere (15).
143
144 We first tested whether preferential attachment or detachment occurs to existing
145 species that have many partners or high partner overlap. Newly arriving AMF species
146 were significantly more likely to interact with plant species that shared fungal
147 partners with many others (Fig. 2A, $P = 1.4 \times 10^{-8}$), but not those with many partners
148 (i.e. high 'degree'; $P = 0.401$) (Table S2). In contrast, plants showed no preferential
149 attachment based on partner overlap (Fig. 2B) or degree of AMF ($P > 0.4$ in both
150 cases, Table S2). However, preferential detachment occurred in both taxa, such that
151 plants and AMF were significantly less likely to be lost from the network during
152 ecosystem retrogression if they interacted with species that had high partner
153 overlap with others in the community ($P < 1.8 \times 10^{-5}$ in both cases; Fig. 2C,D; Table
154 S2).
155
156 As hypothesized previously (11), the disassembly process mirrored the assembly
157 process; the last interactions to form during assembly were the first to be lost during
158 ecosystem retrogression (Fig. 3, $P = 1.64 \times 10^{-9}$). Moreover, the interactions present
159 in sites moving forwards or backwards from the site of peak biomass were nested
160 subsets of those present at that site ($P < 0.001$ in both cases), such that interactions

161 progressively accumulated during progression but were sequentially lost during
162 retrogression. Thus, symmetrical assembly and disassembly processes, either of
163 which could theoretically generate complex network architecture (1, 4, 8, 9), both
164 operated to rapidly generate architecture that did not change significantly
165 throughout ecosystem development (SI Results, Table S3, Fig. S2).
166
167 Although degree and partner overlap were correlated in our networks (Fig. S3), we
168 found no evidence of preferential detachment of plants from AMF of low degree (P =
169 0.577), and AMF taxa even had *increased* detachment probability when they
170 associated with nodes of high degree (P = 0.040), as has been observed in a long-
171 term study of pollination networks (7), and this relation became stronger when
172 partner overlap was also included in the model (Table S2). Moreover, in all our
173 models, partner overlap predicted attachment or detachment probability better
174 than did equivalent models with only degree as the predictor, and its effect
175 remained qualitatively unchanged when degree was also included in the model
176 (Table S2, S4).
177
178 Our findings suggest that both attachment and detachment are key processes in
179 network development and, when combined, the loss or gain of links becomes self-
180 reinforcing (9). We simulated the processes observed here to explore the
181 consequences for network architecture (SI Materials and Methods) and found that
182 both preferential attachment and detachment processes were important for
183 determining and maintaining the nestedness of the network (Fig. S4), a key element
184 of ecological network architecture (1, 12) whereby specialists interact with species
185 that also interact with generalists. Preferential attachment (based on degree or
186 partner overlap) generated networks that were considerably more nested than
187 random, and preferential detachment maintained this nestedness in the face of
188 species extinctions (Fig. S4).
189
190 **Discussion**
191 Obviously species do not have information about the architecture of their interaction
192 networks, so partner overlap must be associated with ecological characteristics that

make species more likely to attract and retain interaction partners. There are several potential, non-exclusive explanations for this attractiveness. The simplest would be if abundant species shared many partners due to a high probability of random encounters. In our dataset, there was a weak correlation between a species' abundance and partner overlap within sites. Moreover, the core of interacting generalists (i.e. the species involved in the majority of interactions in the network, and whose partners overlapped considerably with the rest of the community) was present throughout much of ecosystem development (see dark colors in top left of matrices in Fig. 1), and this ubiquity likely made them a reliable target for newly arriving species. However, causality cannot be inferred from these correlations in our dataset, as attraction of diverse fungal mutualists could equally cause longer-term persistence of plants (30). Most importantly, the relation between plant partner overlap and AMF attachment and detachment probability remained significant after controlling for abundance (SI Results, Table S4). In contrast, the effect of degree was eliminated or even reversed when we controlled for abundance, and the preferential detachment of plants from AMF species with low partner overlap became non-significant when controlling for abundance (SI Results, Table S4).

Therefore, although abundance likely plays some role, the attractiveness of plants with high partner overlap to AMF taxa reflects additional benefits to associating with those species. Plants may benefit from the AMF communities generated by other species (31), and plant-plant competition can be reduced (and plant biomass increased) by high AMF diversity (23). Thus, consortia of plants that are able to share diverse AMF communities with one another may grow better, and therefore have the ability to provide more carbon to AMF symbionts. These groupings may also reflect habitat preference of the species involved, with habitat generalist plant and AMF species interacting tightly during early succession and forest specialists during late succession (25), an hypothesis congruent with findings of partner specificity occurring at the level of ecological groups (14).

The potential benefits of interacting with high-partner-overlap species may be partially offset in newly-arriving plants because seedling performance can be

impaired by the AMF network of large heterospecific plants, which compete for AMF-mediated resources and deplete the nutrient pool (32, 33). Also, the high generality of AMF may mean that there is less variation across species in the extent to which they share plant hosts (evidenced by the range of x-axis values for AMF species being less than half that of plants Fig. 2A,B). Combined, these factors may explain the non-significant effect of AMF degree and partner overlap on plant attachment probability (Fig. 2B).

However, both plant and AMF species were less likely to be lost during retrogression if they interacted with species that had high partner overlap with others in their community (Fig. 2C,D). We hypothesized (based on the benefits described above) that mutually beneficial interactions will involve species with high partner overlap, and we observed that species that preferentially interacted with these core species were significantly more likely to persist during retrogression. The decline in soil P during ecosystem development likely makes plants increasingly dependent on AMF-provided P. Likewise, declining plant photosynthetic rates along the chronosequence (34) could increase competition among AMF for plant-derived carbon. Thus, the need to develop and maintain mutualists and avoid symbiotic 'cheaters' will intensify along the sequence, particularly during retrogression. Over time, both plants and AMF can reduce their resource allocation to less-beneficial partners (22), particularly when resources are scarce (35). The interactions that persist during retrogression may therefore be those that are most mutually beneficial. Previous work has found that species in late-successional plant-AMF networks tend to interact more frequently with a subset of their total range of partners (36), and a viable strategy may thus be to test a number of partners initially, then gradually restrict resource allocation to a subset of these that provide the greatest benefit (35) as resources become limiting. Congruent with this potential strategy, the most generalist plants tended to lose many AMF partners during retrogression (AMF detachment probability increased with host-plant degree). This process could easily occur at the level of plant individuals, but be reflected as a loss of links at the species level.

Finally, if our findings are found to generalize to other ecological networks, they would have several potential applications. First the symmetry of assembly and disassembly processes (Fig. 3) throughout long-term ecosystem development suggests that knowledge of assembly order for a given system could be used to predict the interactions most at risk of extinction, such as in using network information for conservation (37). Species reintroductions during restoration could also follow the reverse order of extinction and replace extinct species with others that fulfill the same network role, or focus on species that share interaction partners with others, and will then attract interactions with any new species that colonize. Similarly, non-native species should interact preferentially with high-partner-overlap species in the network, which could therefore be a focus for biosecurity monitoring to detect invasions early.

It is impossible to fully understand the architecture of complex networks in isolation from the dynamic processes that generate and maintain them (4). We have shown empirically that both preferential attachment and detachment underpinned the development of an ecological network under changing abiotic conditions. These symmetrical, self-reinforcing processes can generate and maintain important features of interaction network architecture (1, 4, 8, 9), and thereby link species colonization and extinction to emergent and potentially stabilizing (1, 2) ecosystem properties.

Materials and Methods

Dataset

We generated networks of interactions between vascular plants and arbuscular mycorrhizal fungi (AMF) using data from a study that examined AMF beta diversity and the importance of soil age vs. plant host for explaining AMF community structure (15). Sampling and sequencing methods can be found in that study or in the SI Materials and Methods, but we summarise the key points here. Sampling was conducted along the Franz Josef soil chronosequence, on the southern west coast of the South Island, New Zealand. An important feature of the Franz Josef chronosequence, which led us to select this site, is that strong soil nutrient gradients

(SI Materials and Methods) are associated with pronounced shifts in ecological community composition, structure and function, such that ecosystem development exhibits a clear progressive phase up to the 12,000 year old surface at which peak tree biomass occurs (we treated this as the assembly phase), and a retrogressive phase thereafter in which tree basal area (biomass) declines about three-fold (29, 38) (the disassembly phase). We sampled fungal communities on roots at ten surfaces of the following ages (in years): <5, 15, 70, 290, 500, 1000, 5000, 12,000, 60,000, 120,000 (SI Materials and Methods; Table S1).

At each site we sampled 50 root fragments, which then underwent a molecular analysis to identify the plant species, as well as any AMF OTUs present inside the root (see (15) or SI Materials and Methods). We did not assign weights to these links, as the hypotheses we test here relate to the initial formation of interactions, rather than their strength or frequency once formed.

Data analysis

We hypothesized that species entering the network for the first time during the progressive phase would associate non-randomly with other existing species based on their position within the network (i.e. preferential attachment (4)). We also hypothesized that the same would occur during the disassembly of the network, such that the probability of species going locally extinct from the network would depend on the network position of species with which they associate (i.e. preferential detachment (8, 10)). We tested for preferential attachment during the progressive phase (5 - 12,000 year-old) and preferential detachment during the retrogressive phase (12,000 – 120,000 year-old), representing respectively the assembly and disassembly of the network. We then examined the appearance (attachment) of new species in the network during assembly, and disappearance (detachment) of species during disassembly. A species was deemed to have attached during the progressive phase when it first appeared in the chronosequence. During the progressive phase, once a species had attached (i.e. a link was formed), it was deemed to remain part of the network for the remainder of ecosystem progression. This ensured that any species that appeared, disappeared then reappeared during

320 the progressive phase was not counted twice, which would give any species-specific
321 interaction preferences of these species a disproportionate weighting in analyses.
322 Finally, it prevented underestimation of degree or partner overlap due to imperfect
323 sampling of the network in any given stage. Similarly, detachment was deemed to
324 have occurred during the retrogressive phase when a species that had been present
325 during the progressive phase was absent from a given site and all remaining sites
326 along the sequence. Note that, because by definition attachment and detachment
327 processes must occur during the interval between two chronosequence stages (e.g.,
328 an interaction was present in site B that was not present in A), we treated the 12,000
329 year-old site (which represented the community peak in diversity and biomass) as
330 the 'peak' community, comprising the last stage of assembly and the first stage from
331 which disassembly occurred.
332
333 *Preferential attachment and detachment*
334 We analyzed preferential attachment and detachment processes using generalized
335 linear mixed effects models with binomial errors and the canonical logit link function,
336 conducted in the lme4 package (39) in R (40). We used separate models to test for
337 attachment processes during progression vs. detachment processes during
338 retrogression, and for plants vs. AMF. The response variable in each model was
339 binary, whereby each existing species in the network for each site was coded with a
340 value of 0 (a newly-arriving species did not attach to it, or a species did not detach
341 from it, in that site) or 1 (a new species attached to or detached from the species in
342 that site). Site (surface along the chronosequence) was included as a random factor,
343 such that preferential attachment was tested according to the relative network roles
344 of the various species within a site, rather than comparing species across sites, which
345 could be influenced by differences in the sizes of networks. The fixed predictor
346 variable was either degree or centrality (defined below).
347
348 To measure overlap in the use of interaction partners among species at a given
349 trophic level, we used closeness centrality (hereafter 'centrality', defined in Fig. S1)
350 in the unipartite projection of the bipartite interaction network (41). Centrality is
351 often correlated with degree (42), but carries additional information by measuring

352 the number of links from a focal species to all others in the network (not just
353 immediate neighbors), and has been used as a measure of species' importance (42)
354 or functional specialization (43) in mutualistic networks. In the unipartite projection,
355 species at a given trophic level are linked if they share an interaction partner (Fig. S1),
356 so high centrality indicates that a species shares many partners with other species
357 that also share partners with many others. In contrast, species with low centrality
358 interact with partners that are not used by the dominant consortium of tightly-
359 interacting plants and AMF. Although centrality may be implicitly used to infer the
360 nature of flows through a network (e.g. paths vs. walks, replication vs. spread), we
361 do not make any assumption about the nature of flows, if any, in the plant-AMF
362 network. Rather, we use closeness centrality simply as a measure of the extent to
363 which different species share interaction partners within a trophic level. Centrality
364 was calculated in the 'sna' package (44) in R, scaled within a given network (i.e.
365 within each site).
366
367 We tested whether attachment to a node during assembly, or detachment from a
368 node during disassembly, depended on that node's centrality (Fig. S1) or degree (the
369 number of partners with which the species interacts, normalized within networks of
370 a given site age). We used the centrality/degree of a node in the chronosequence
371 stage immediately prior to that in which the new node attached or an existing node
372 detached. This allowed us to compare the fit of models with centrality vs. degree as
373 the predictor using the Akaike Information Criterion (AIC). Thus, the predictor
374 variable in each model was either the degree or centrality of each existing species in
375 the site, to which newly-arriving species either attached vs. did not, or detached vs.
376 did not. For completeness, we also ran models with both of these predictors, to
377 determine if any potential collinearity qualitatively altered their separate effect.
378 None of our models showed any signs of overdispersion. We repeated these
379 analyses controlling for species abundances in case sampling effort generated any
380 spurious effects (see Controlling for the effect of species abundances in SI Materials
381 and Methods).
382

383 We omitted from this analysis any links representing new species attaching to other
384 newly-arriving species, because we could not ascribe a value of network position for
385 those species to use as the predictor variable. However, these pairings among two
386 newly-arriving species were rare, and the species involved typically also interacted
387 with other species already present in the network. Across all sites, 20 newly-arriving
388 plant species were associated with newly-arriving AMF, and of these, 16 species also
389 attached to AMF species that were already present in the network, for which
390 network position could be calculated. Similarly, of the 15 newly-arriving AMF species
391 that attached to newly-arriving plants, 8 also attached to existing species.
392
393 *Arrival and extinction order*
394 We tested whether the arrival and disappearance (extinction) order of links in the
395 ecological network through time occurred at random, or whether links that
396 appeared first during progression were last to be lost from the network during
397 retrogression. To test this, we analyzed the arrival and extinction order of each link
398 (i.e. each association between a mycorrhizal species and a plant species). This
399 analysis included both links of newly-arriving species (as in the preferential
400 attachment analysis above) and links that formed among existing species. Arrival
401 order was defined as the rank age of the site at which the interaction was first
402 observed; e.g. an interaction observed at the earliest (< 5 year-old) site was given a
403 value of 1, whereas an interaction first observed at the 1,000 year old site (6th along
404 the sequence) was given a value of 6. We treated the network at the site of peak
405 plant biomass (29) (12,000 years old) as the end point of the assembly phase, then
406 examined the order in which interactions were lost during the retrogressive phase
407 following this peak (i.e. the extinction order). Extinction order was defined, in the
408 same way as arrival order, as the first site following the peak biomass site in which
409 an interaction was not observed. For example, an interaction that was present at the
410 peak biomass site but not the latter two sites was given an extinction order of 1, an
411 interaction that was present at the peak biomass site and both of the remaining sites
412 was given an extinction order of 3, etc. For the analysis we used only those
413 interactions that were present in the peak biomass site, in order to be conservative;
414 had we simply used the arrival order and extinction order (last site in which an

interaction occurred) of all interactions across the sequence, this would have biased us towards finding a significant result, because any interactions that only appeared once along the sequence, or appeared early and were gone by the site of peak biomass, would have generated an automatic correlation between their arrival and extinction orders.

Thus, our analysis focused on the network of the peak biomass site and tested whether the order in which interactions came into the network was correlated with the order in which they were lost from the network. We tested for a relationship between arrival and extinction order using a simple regression, with extinction order as the response variable and arrival order as the predictor variable, and each interaction (plant-mycorrhizal combination) was a replicate. There remained the possibility that any observed relationship could be driven by interactions that appeared only in the site of peak biomass, and hence would be last to arrive and first to go extinct. To account for this, we re-ran the analysis after removing interactions that were only present in the site of peak biomass.

A negative correlation between arrival and extinction order of interactions would suggest a gradual accumulation of interactions in the network up until the site of peak biomass, followed by a progressive loss of interactions. This would be expected to generate a pattern whereby the peak biomass site has a set of interactions, of which progressively older or younger sites have decreasing subsets. To test for such a pattern, we generated two matrices in which we ranked the sites according to their age (rows), either becoming progressively older or younger than the site of peak biomass, which was in the top row. Cells of the matrices depicted the presence or absence of each pairwise plant-AMF association (columns). We tested each matrix for nestedness, using the nestedness metric based on overlap and decreasing fill (NODF), with 999 permutations and a swap algorithm, using the oecosimu function in the vegan (45) package for R (40).

<u>Simulations</u>

To explore the consequences of preferential attachment and detachment based on centrality vs. degree, we conducted a set of simulations of network assembly and disassembly scenarios (more detail provided in SI Materials and Methods). At each time step, newly-arriving plant or AMF species would interact with one existing species, with a probability proportional to the existing species' degree (i.e. the Barabasi and Albert model (4)) or partner overlap (closeness centrality). We also ran a third scenario whereby attachment was random (equally probable attachment to any existing species), to provide a null point of comparison.

This assembly phase continued until networks contained 50 species of plant and 50 of AMF. Subsequently, each network was subjected to a disassembly phase, using the same scenario (degree-based, centrality-based or random) as was used during that network's assembly. Alternating plant and AMF species were removed (i.e. went extinct) with a probability that was inversely proportional to the degree or closeness centrality of the species with which they interacted, such that species that interacted with species of high degree or high centrality were less likely to go extinct. As with the assembly phase, we ran a scenario of the disassembly phase whereby extinction was random.

Each scenario of the assembly and disassembly phases was run for 1000 replicates (each comprising multiple time steps). At each time step within each replicate, after species arrived or went extinct, we recorded the nestedness of the network using NODF, calculated using the nestednodf function in the vegan package (45) for R. Nestedness is a common feature of mutualistic networks (46), which has also been observed recently in plant-mycorrhizal networks (12) and has been shown to increase the persistence of networks (1, 2). We scaled the observed NODF by the distribution of NODF values obtained by randomizing the adjacency matrix using a null model (SI Materials and Methods).

References

1. Bastolla U*, et al.* (2009) The architecture of mutualistic networks minimizes competition and increases biodiversity. *Nature* 458(7241):1018-U1091.
2. Thebault E & Fontaine C (2010) Stability of Ecological Communities and the Architecture of Mutualistic and Trophic Networks. *Science* 329(5993):853-856.
3. Thompson RM*, et al.* (2012) Food webs: reconciling the structure and function of biodiversity. *Trends in ecology & evolution*.
4. Barabási A-L & Albert R (1999) Emergence of scaling in random networks. *Science* 286(5439):509-512.
5. Jordano P, Bascompte J, & Olesen JM (2003) Invariant properties in coevolutionary networks of plant-animal interactions. *Ecology letters* 6(1):69-81.
6. Olesen JM, Bascompte J, Elberling H, & Jordano P (2008) Temporal dynamics in a pollination network. *Ecology* 89(6):1573-1582.
7. Burkle LA, Marlin JC, & Knight TM (2013) Plant-pollinator interactions over 120 years: loss of species, co-occurrence, and function. *Science* 339(6127):1611-1615.
8. Salathé M, May RM, & Bonhoeffer S (2005) The evolution of network topology by selective removal. *Journal of the Royal Society Interface* 2(5):533-536.
9. König M, Tessone C, & Zenou Y (2012) Nestedness in Networks: A Theoretical Model and Someapplications. *SIEPR Discussion Papers* 11(005):1-61.
10. Aizen MA, Sabatino M, & Tylianakis JM (2012) Specialization and Rarity Predict Nonrandom Loss of Interactions from Mutualist Networks. *Science* 335(6075):1486-1489.
11. Bascompte J & Stouffer DB (2009) The assembly and disassembly of ecological networks. *Philosophical Transactions of the Royal Society B-Biological Sciences* 364(1524):1781-1787.
12. Montesinos-Navarro A, Segarra-Moragues JG, Valiente-Banuet A, & Verdu M (2012) The network structure of plant-arbuscular mycorrhizal fungi. *New Phytologist* 194(2):536-547.
13. Brundrett MC (2009) Mycorrhizal associations and other means of nutrition of vascular plants: understanding the global diversity of host plants by resolving conflicting information and developing reliable means of diagnosis. *Plant and Soil* 320(1-2):37-77.
14. Öpik M, Metsis M, Daniell T, Zobel M, & Moora M (2009) Large‐scale parallel 454 sequencing reveals host ecological group specificity of arbuscular mycorrhizal fungi in a boreonemoral forest. *New Phytologist* 184(2):424-437.
15. Martínez‐García LB, Richardson SJ, Tylianakis JM, Peltzer DA, & Dickie IA (2015) Host identity is a dominant driver of mycorrhizal fungal community composition during ecosystem development. *New Phytologist* 205(4):1565-1576.
16. Vályi K, Rillig MC, & Hempel S (2015) Land‐use intensity and host plant identity interactively shape communities of arbuscular mycorrhizal fungi in roots of grassland plants. *New Phytologist* 205(4):1577-1586.

17. Powell JR*, et al.* (2015) Deterministic processes vary during community assembly for ecologically dissimilar taxa. *Nature communications* 6.
18. Krüger M*, et al.* (2015) The rise and fall of arbuscular mycorrhizal fungal diversity during ecosystem retrogression. *Mol. Ecol.* 24(19):4912-4930.
19. Encinas‐Viso F, Alonso D, Klironomos JN, Etienne RS, & Chang ER (2015) Plant‐mycorrhizal fungus co‐occurrence network lacks substantial structure. *Oikos*.
20. Newman EI (1988) Mycorrhizal links between plants: their functioning and ecological significance. *Advances in Ecological Research* 18:243-270.
21. Simard SW & Durall DM (2004) Mycorrhizal networks: a review of their extent, function, and importance. *Canadian Journal of Botany* 82(8):1140-1165.
22. Kiers ET*, et al.* (2011) Reciprocal rewards stabilize cooperation in the mycorrhizal symbiosis. *science* 333(6044):880-882.
23. Wagg C, Jansa J, Stadler M, Schmid B, & Van Der Heijden MGA (2011) Mycorrhizal fungal identity and diversity relaxes plant-plant competition. *Ecology* 92(6):1303-1313.
24. Ehinger M, Koch AM, & Sanders IR (2009) Changes in arbuscular mycorrhizal fungal phenotypes and genotypes in response to plant species identity and phosphorus concentration. *New Phytologist* 184(2):412-423.
25. Davison J, Öpik M, Daniell TJ, Moora M, & Zobel M (2011) Arbuscular mycorrhizal fungal communities in plant roots are not random assemblages. *FEMS Microbiology Ecology* 78(1):103-115.
26. Horn S, Caruso T, Verbruggen E, Rillig MC, & Hempel S (2014) Arbuscular mycorrhizal fungal communities are phylogenetically clustered at small scales. *The ISME journal* 8(11):2231-2242.
27. Gómez JM, Verdú M, & Perfectti F (2010) Ecological interactions are evolutionarily conserved across the entire tree of life. *Nature* 465(7300):918-921.
28. Peltzer DA*, et al.* (2010) Understanding ecosystem retrogression. *Ecological Monographs* 80(4):509-529.
29. Richardson SJ, Peltzer DA, Allen RB, McGlone MS, & Parfitt RL (2004) Rapid development of phosphorus limitation in temperate rainforest along the Franz Josef soil chronosequence. *Oecologia* 139(2):267-276.
30. Scheublin TR, Van Logtestijn RSP, & Van Der Heijden MGA (2007) Presence and identity of arbuscular mycorrhizal fungi influence competitive interactions between plant species. *Journal of Ecology* 95(4):631-638.
31. Bever JD (2002) Negative feedback within a mutualism: host–specific growth of mycorrhizal fungi reduces plant benefit. *Proceedings of the Royal Society of London B: Biological Sciences* 269(1509):2595-2601.
32. Kytöviita MM, Vestberg M, & Tuomi J (2003) A test of mutual aid in common mycorrhizal networks: established vegetation negates benefit in seedlings. *Ecology* 84(4):898-906.
33. Janoušková M, Rydlová J, Püschel D, Száková J, & Vosátka M (2011) Extraradical mycelium of arbuscular mycorrhizal fungi radiating from large plants depresses the growth of nearby seedlings in a nutrient deficient substrate. *Mycorrhiza* 21(7):641-650.

34. Whitehead D, *et al.* (2005) Photosynthesis and reflectance indices for rainforest species in ecosystems undergoing progression and retrogression along a soil fertility chronosequence in New Zealand. *Oecologia* 144(2):233-244.
35. Bever JD (2015) Preferential allocation, physio‐evolutionary feedbacks, and the stability and environmental patterns of mutualism between plants and their root symbionts. *New Phytologist* 205(4):1503-1514.
36. Bennett AE, *et al.* (2013) Arbuscular mycorrhizal fungal networks vary throughout the growing season and between successional stages. *PloS one* 8(12):e83241.
37. Tylianakis JM, Laliberté E, Nielsen A, & Bascompte J (2010) Conservation of species interaction networks. *Biological Conservation* 143:2270-2279.
38. Wardle D, Bardgett R, Walker L, Peltzer D, & Lagerström A (2008) The response of plant diversity to ecosystem retrogression: evidence from contrasting long-term chronosequences. *Oikos* 117:93 -103.
39. Bates D, Maechler M, Bolker B, & Walker S (2014) lme4: Linear mixed-effects models using Eigen and S4), R package version 1.0-6.
40. Team RC (2013) R: A language and environment for statistical computing. (R Foundation for Statistical Computing, Vienna Austria), 3.0.1.
41. Gómez JM & Perfectti F (2012) Fitness consequences of centrality in mutualistic individual-based networks. *Proceedings of the Royal Society B: Biological Sciences* 279(1734):1754-1760.
42. Martín González AM, Dalsgaard B, & Olesen JM (2010) Centrality measures and the importance of generalist species in pollination networks. *Ecological Complexity* 7(1):36-43.
43. Dalsgaard B, *et al.* (2008) Pollination networks and functional specialization: a test using Lesser Antillean plant–hummingbird assemblages. *Oikos* 117(5):789-793.
44. Butts CT (2014) sna: Tools for Social Network Analysis.), R package version 2.3-2.
45. Oksanen J, *et al.* (2008) vegan: Community Ecology Package (http://cran.r-project.org/).
46. Bascompte J, Jordano P, Melian CJ, & Olesen JM (2003) The nested assembly of plant-animal mutualistic networks. *Proceedings of the National Academy of Sciences of the United States of America* 100(16):9383-9387.
47. Stevens PR (1968) A chronosequence of soils near the Franz Josef Glacier. PhD thesis (University of Canterbury, New Zealand).
48. Walker T & Syers J (1976) The fate of phosphorus during pedogenesis. *Geoderma* 15(1):1-19.
49. Allison V, Condron L, Peltzer D, Richardson S, & Turner B (2007) Changes in enzyme activities and soil microbial community composition along carbon and nutrient gradients at the Franz Josef chronosequence, New Zealand. *Soil Biology and Biochemistry* 39(7):1770-1781.
50. Jangid K, Whitman WB, Condron LM, Turner BL, & Williams MA (2013) Progressive and retrogressive ecosystem development coincide with soil bacterial community change in a dune system under lowland temperate rainforest in New Zealand. *Plant and soil* 367(1-2):235-247.

51. Dickie IA*, et al.* (2013) Mycorrhizas and mycorrhizal fungal communities throughout ecosystem development. *Plant and Soil* 367(1-2):11-39.
52. Lambers H, Raven JA, Shaver GR, & Smith SE (2008) Plant nutrient-acquisition strategies change with soil age. *Trends in Ecology & Evolution* 23(2):95-103.
53. Turner S*, et al.* (2014) Mineralogical impact on long-term patterns of soil nitrogen and phosphorus enzyme activities. *Soil Biology and Biochemistry* 68:31-43.
54. Richardson SJ, Peltzer DA, Allen RB, & McGlone MS (2010) Declining soil fertility does not increase leaf lifespan within species: evidence from the Franz Josef chronosequence, New Zealand. *New Zealand Journal of Ecology* 34(3):306-310.
55. Holdaway RJ, Richardson SJ, Dickie IA, Peltzer DA, & Coomes DA (2011) Species- and community-level patterns in fine root traits along a 120 000-year soil chronosequence in temperate rain forest. *Journal of Ecology* 99(4):954-963.
56. Wardle DA, Walker LR, & Bardgett RD (2004) Ecosystem properties and forest decline in contrasting long-term chronosequences. *Science* 305:509-513.
57. Doblas-Miranda E, Wardle DA, Peltzer DA, & Yeates GW (2008) Changes in the community structure and diversity of soil invertebrates across the Franz Josef Glacier chronosequence. *Soil Biology and Biochemistry* 40(5):1069-1081.
58. Wardle P (1991) *Vegetation of New Zealand* (CUP Archive).
59. Öpik M & Moora M (2012) Missing nodes and links in mycorrhizal networks. *New Phytologist* 194(2):304-306.
60. Simon L, Lalonde M, & Bruns T (1992) Specific amplification of 18S fungal ribosomal genes from vesicular-arbuscular endomycorrhizal fungi colonizing roots. *Applied and Environmental Microbiology* 58(1):291-295.
61. Lee J, Lee S, & Young JPW (2008) Improved PCR primers for the detection and identification of arbuscular mycorrhizal fungi. *FEMS Microbiology Ecology* 65(2):339-349.
62. Dickie I & FitzJohn R (2007) Using terminal restriction fragment length polymorphism (T-RFLP) to identify mycorrhizal fungi: a methods review. *Mycorrhiza* 17(4):259-270.
63. van Dorst J*, et al.* (2014) Community fingerprinting in a sequencing world. *FEMS microbiology ecology* 89(2):316-330.
64. White TJ, Bruns T, Lee S, & Taylor J (1990) Amplification and direct sequencing of fungal ribosomal RNA genes for phylogenetics. *PCR protocols: a guide to methods and applications* 18:315-322.
65. Taberlet P, Gielly L, Pautou G, & Bouvet J (1991) Universal primers for amplification of three non-coding regions of chloroplast DNA. *Plant molecular biology* 17(5):1105-1109.
66. Trewick S*, et al.* (2002) Polyploidy, phylogeography and Pleistocene refugia of the rockfern Asplenium ceterach: evidence from chloroplast DNA. *Mol. Ecol.* 11(10):2003-2012.
67. Wirta HK*, et al.* (2014) Complementary molecular information changes our perception of food web structure. *Proceedings of the National Academy of Sciences* 111(5):1885-1890.

68. Toju H, Guimarães PR, Olesen JM, & Thompson JN (2014) Assembly of complex plant–fungus networks. *Nature communications* 5.
69. Caruso T, Rillig MC, & Garlaschelli D (2012) On the application of network theory to arbuscular mycorrhizal fungi–plant interactions: the importance of basic assumptions. *New Phytologist* 194(4):891-894.
70. Graham J & Eissenstat D (1994) Host genotype and the formation and function of VA mycorrhizae. *Plant and Soil* 159(1):179-185.
71. Nguyen NH, Smith D, Peay K, & Kennedy P (2014) Parsing ecological signal from noise in next generation amplicon sequencing. *New Phytologist*.
72. Hurst J & Allen R (2007) *A permanent plot method for monitoring indigenous forests – Field protocols* (Landcare Research, Lincoln, New Zealand), (Research L).
73. Albrecht M, Riesen M, & Schmid B (2010) Plant-pollinator network assembly along the chronosequence of a glacier foreland. *Oikos* 119(10):1610-1624.
74. Fahimipour AK & Hein AM (2014) The dynamics of assembling food webs. *Ecology Letters* 17(5):606-613.
75. Kuznetsova A, Brockhoff P, & Christensen R (2013) lmerTest: Tests for random and fixed effects for linear mixed effect models (lmer objects of lme4 package). *R package version*:2.0-0.

Acknowledgements

We thank P.J. Bellingham, T. Fukami, J.H. Jones, S. Pawar, D.B. Stouffer and members of the Tylianakis/Stouffer lab for critical discussions and comments on the manuscript. N. Bolstridge and C. Mitchel provided valuable lab assistance. The research was funded by Core funding for Crown Research Institutes from the New Zealand Ministry of Business, Innovation and Employment's Science and Innovation Group, and a Rutherford Discovery Fellowship to JMT. This paper is a contribution to Imperial College's Grand Challenges in Ecosystems and the Environment initiative.

Author contributions

J.M.T. and I.A.D. designed the study, in discussion with all other authors. L.B.M.-G. and I.A.D. conducted molecular analyses. J.M.T. conducted statistical analyses. S.J.R. and D.A.P. collected plant abundance data. All authors contributed to field sampling and writing of the manuscript.

Author information

The authors declare no competing financial interests. Correspondence and requests for materials should be addressed to J.M.T. (jason.tylianakis@canterbury.ac.nz).

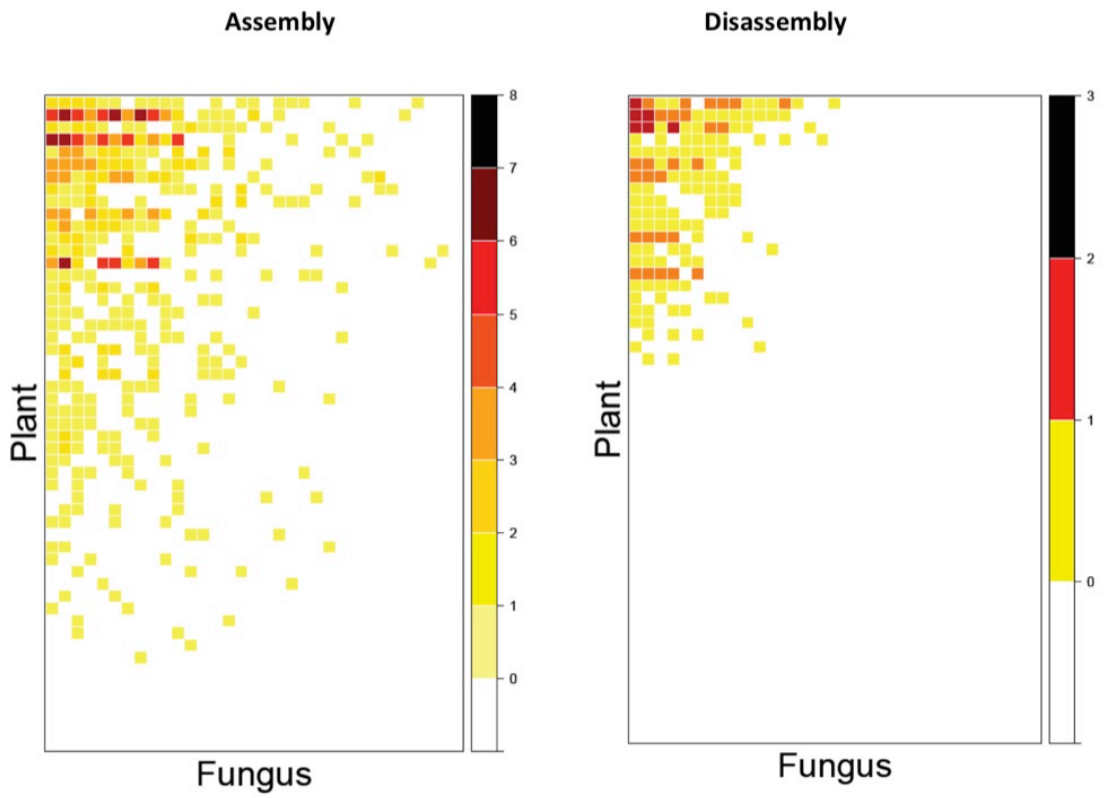

Figure 1: Plant-mycorrhizal association matrices during assembly (N = 8 sites) and disassembly (i.e. retrogressive, N = 3 sites) phases of ecosystem development. Darker colours indicate that the plant-mycorrhizal association was present in a greater number of sites (i.e. it formed early during assembly or persisted during retrogression). The network is significantly nested (see SI Results), whereby specialists interact with proper subsets of the species that interact with generalists.

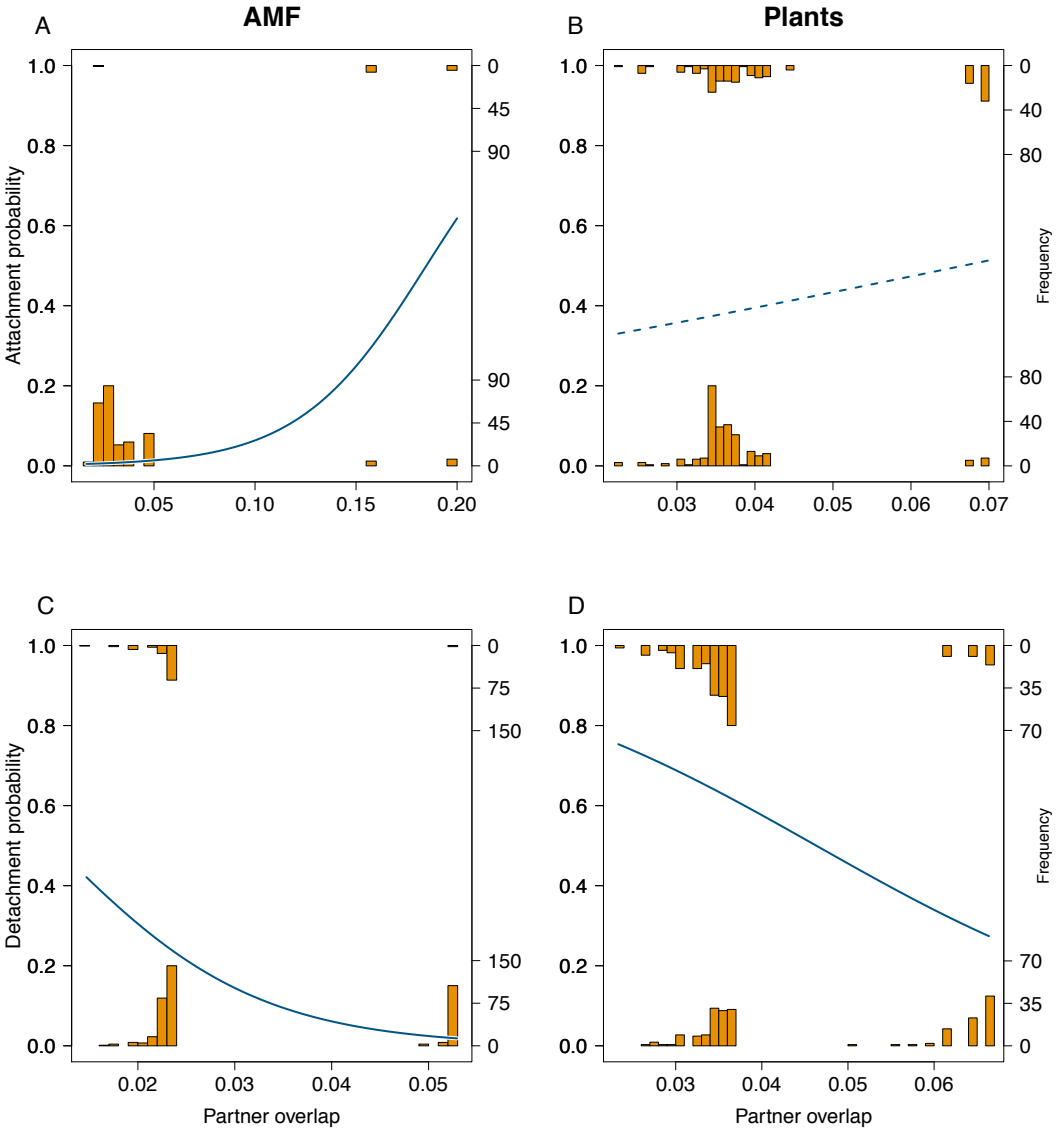

Figure 2: Probability (left vertical axis) that a new A,C) arbuscular mycorrhizal fungus (AMF), or B,D) plant entering the network will interact with an existing species during assembly (top), or detach from a species during disassembly (bottom) as a function of that species interaction-partner overlap with others of its trophic level (measured as closeness centrality of the unipartite projection, see Fig. S1). Histograms top and bottom of each graph represent the frequencies (right vertical axis) of ones and zeroes respectively in the raw data. Trend lines are based on inverse-linked coefficients of a binomial linear mixed effects model with chronosequence stage (plant-mycorrhizal network) or year (arms trade network) as a random effect. Solid lines were statistically significant ($P < 0.005$ in all cases), dashed line was not significant at alpha = 0.05.

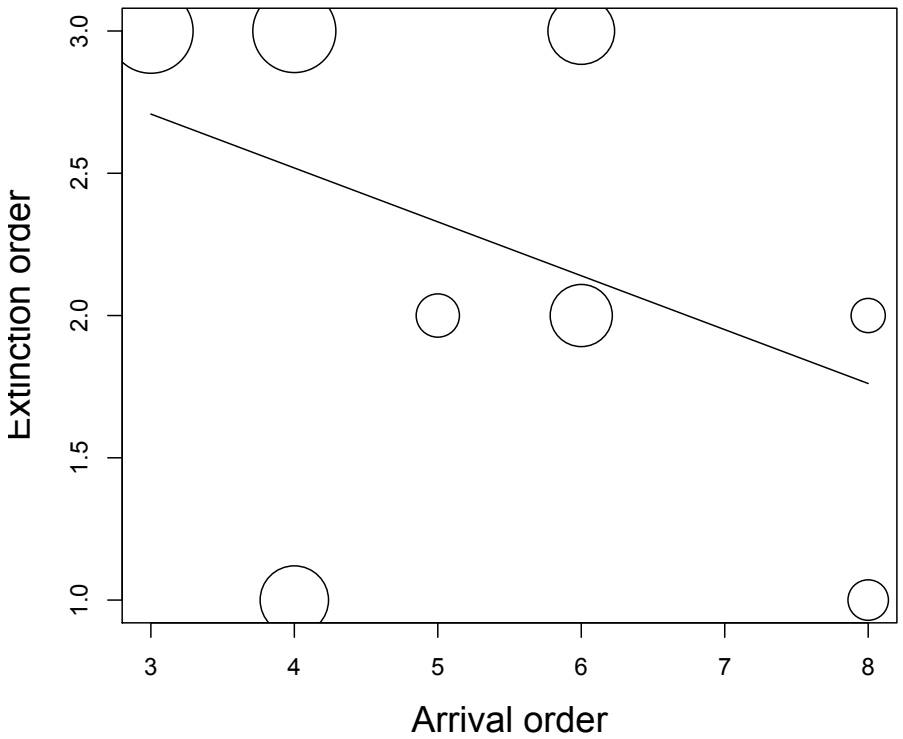

Figure 3: The relationship between the order in which plant-AMF interactions (network 'links') were formed (arrival order) and that in which they were lost (extinction order). Larger circles indicate more overlapping data points. There was a significant negative association between the formation and disappearance order of interactions ($F_{1,269} = 39$, $P < 0.0001$), such that the last interactions to form during network assembly were the first to be lost during disassembly. This analysis only included interactions that were present at the site of peak biomass (arrival order 8), so was not confounded by interactions that appeared in only one site (i.e. arrived and went 'extinct' instantly). The relationship was also not simply driven by interactions that appeared only in the site of peak biomass, as it remained significant even when these data points were removed ($F_{1,245} = 5.38$, $P < 0.022$).

SI Materials and Methods

Study site

We sampled interactions between vascular plants and arbuscular mycorrhizal fungi (AMF) along the Franz Josef soil chronosequence, on the southern west coast of the South Island, New Zealand. The sites are schist outwash surfaces that have been exposed during glacial retreat, and span a range of ages (since exposure) from more than 120,000 years to the present. An important feature of the Franz Josef chronosequence, which led us to select this site, is that strong soil nutrient gradients) are associated with pronounced shifts in ecological community composition, structure and function, such that ecosystem development exhibits a clear progressive phase up to the 12,000 year old surface at which peak tree biomass occurs (we treated this as the assembly phase), and a retrogressive phase thereafter in which tree basal area (biomass) declines about three-fold (29, 38) (the disassembly phase). We sampled fungal communities on roots at ten surfaces of the following ages (in years): <5, 15, 70, 290, 500, 1000, 5000, 12,000, 60,000, 120,000 (Table S1).

The sampling sites occur between the terminus of the Franz Josef glacier (43.45° S, 170.17° E) and the coast of central western South Island (43.25° S,170.19° E) (29, 47). The current climate is highly oceanic and mean annual temperature (1926–1975) at the valley mouth is 10.8ºC . Precipitation is ca. 6.5m for first seven sites of the sequence, which are within the glacier valley, and ca. 3.5m for the last three sites that lie between the valley mouth and the coast. Precipitation falls evenly throughout the year.

Inorganic phosphorus (P) is initially high (> 800 mg/kg), but declines to ca. 100 mg/kg by the oldest stage (29). Declining phosphorus is associated with a shift from plant-available mineral forms to organic forms. Mineral soil nitrogen and carbon concentrations are initially negligible (<0.1%) but increase rapidly during the first 100 years of ecosystem development in association with nitrogen-fixing species and accumulating tree biomass; both reach peak concentrations at 500 years and decline slowly thereafter (29, 38).

We sampled fungal communities on roots at ten surfaces of the following ages (in years): <5, 15, 70, 290, 500, 1000, 5000, 12,000, 60,000, 120,000. These sites are based on those used by Richardson et al. (29), with three differences: the addition of a <5-year old surface at the glacier forefront and a 1000-year old site, and a 12,000 year old site that was used in the original description (48) of the chronosequence, in lieu of Richardson et al's (29) 12 kyr. site. Our sites ranged from initial post-glacial primary succession (gravel bed with sparse grasses and subshrubs, highly nitrogen limited with abundant phosphorus) through the assembly of a temperate rainforest (soils ca. 12,000 years old with maximal aboveground biomass limited primarily by P) and ultimately retrogressive phases (the two sites ≥60 kyr old having severe nutrient depletion through pedogenic processes) (29).

Forests along the chronosequence, and in the region generally, are formed by associations of broadleaved evergreen angiosperm and long-lived coniferous (arbuscular mycorrhizal Podocarpaceae) tree species with abundant tree ferns, lianas and ground ferns (29). Endemic evergreen angiosperms dominate the youngest sites (from 5 to 290 yr age), and thereafter are replaced by major canopy dominant tree species, primarily Podocarpaceae; these dominate the plant community throughout the remainder of the chronosequence. Tree ferns occur across all the sites except the oldest (120,000 yr) (29); grasses and ericaceous shrubs are almost absent from the chronosequence, but do form a minor component of the vegetation on the 15 yr and oldest sites respectively.

Strong shifts also occur in belowground properties and biota along this sequence, mirroring the co-ordinated shifts in nutrients, community composition and ecological processes throughout ecosystem development. Soil microbial communities decline in diversity and richness along the sequence, and compositionally shift from bacterial-dominated to fungal-dominated (49). In addition, some bacterial phyla are common throughout the sequence (e.g., Actinomycetes and alpha-Proteobacteria), whereas other phyla decline over time (e.g., Bacilli, beta-Proteobacteria, and Bacteriodetes (50)). Similarly, mycorrhizal fungi are dominated by arbuscular species

801 throughout. Orchid mycorrhizas are present throughout the sequence, but are
802 extremely rare; ericoid mycorrhizas are present primarily on the oldest, retrogressive
803 stage (51, 52) (although the ericaceous shrub *Gaultheria* is also present at the 15
804 year old site); and a plant species capable of forming ectomycorrhizas
805 (*Leptospermum scoparium*) is present at the oldest site, but no ectomycorrhizal
806 roots have been observed. In addition, soil microbes and fungi are an increasingly
807 important pool of P whereby the majority of available (non-occluded) P is retained in
808 the soil microbial biomass during ecosystem retrogression (53). Activities of the soil
809 microbial biomass are coordinated such that investment in phosphorous acquisition
810 increases along the sequence, as demonstrated by a four-fold increase in the major
811 enzymes used to process phosphorus (phosphomonoesterase and phophodiesterase
812 (49, 53)).
813
814 Plant functional leaf and root traits show a co-ordinated shift predictably towards an
815 increasingly conservative resource-use strategy with increasing surface age, both
816 within widespread species and through species turnover (29, 54, 55). The sites in the
817 early (progressive) phase represent the stages typical of ecosystem succession,
818 whereas the two oldest sites are considered retrogressive (28, 29, 56) due to soil
819 nutrient limitation.
820
821 Changes in the diversity, abundance and composition of litter and soil-dwelling
822 invertebrates are less well understood. The abundance of microbial-feeding and
823 omnivorous nematodes and copepods show unimodal responses along the sequence
824 in soil, but more complex responses in the litter layer (57). Richness and diversity of
825 both nematodes and macroinvertebrates differ significantly among stages or sites,
826 but do not shift consistently throughout ecosystem development. Acari abundance is
827 biomodal, peaking in early and mid stages of the sequence, whereas diversity
828 increases throughout. In contrast, Collembola abundance and diversity are both
829 bimodal, peaking at the earliest and maximal biomass stages. These results suggest
830 that soil microbial community composition and activity are coordinated along the
831 sequence, but that other soil biota, such as invertebrates, have more complex
832 responses; these are likely driven by the relative strength and importance of top-

833 down vs. bottom-up regulation of these taxa (56), but these processes have not yet
834 been investigated.
835
836 *Sampling*
837 At each site we sampled 50 root fragments of 10 to 20 cm length from the organic or
838 mineral layer at a depth of 10-30 cm, where the majority of fine roots occur (p.43 in
839 (58)), with each sample spaced 2 m apart along two parallel 50 m transects. This
840 depth allowed consistent sampling across all sites (all sites had roots at this depth)
841 and high replication with minimal site disturbance, but we note that the root and
842 fungal community below 30 cm was not included. Thus, the frequency with which
843 plant species appeared in our samples should reflect their relative abundance (or at
844 least belowground biomass from 10-30 cm) in the site (59), congruent with transect
845 samples frequently used to sample pollination or host-parasitoid networks (6, 10).
846 Although species density per unit space (and therefore sampling probability of each
847 species) may change along the sequence, our analyses do not compare sites with
848 each other. Rather, we make comparisons within sites of attachment and
849 detachment probability based on the network role of species. We took the same
850 number of samples from each depth (10, 20 or 30 cm) at each site, randomly
851 positioned along each transect, to ensure coverage of different root zones. Roots
852 were thoroughly washed with tap water to remove any attached soil, then freeze-
853 dried overnight. Visual inspection suggested that tap water washing was effective at
854 removing all soil. Additionally, at each site, leaves from the most representative
855 plants were identified, collected and frozen for molecular analysis. During this
856 process both root and leaf samples were kept cold (5°C). Root samples then
857 underwent a molecular analysis to identify the plant species, as well as any AMF
858 OTUs present inside the root (see Justification of our Sequencing Approach below).
859 We did not assign weights to the links, as the hypotheses we test here relate to the
860 initial formation of interactions, rather than their strength or frequency once formed.
861
862 *Molecular analysis*
863 Arbuscular mycorrhizal fungal (Glomeromycota) DNA was amplified using the
864 universal eukaryotic primer NS31 (60) with the fluorochrome label VIC and the

865 arbuscular mycorrhizal fungal specific primer AML2 (61) labeled with 6FAM, cleaned,
866 and analyzed using terminal restriction fragment length polymorphism (T-RFLP (62)).
867 Network analysis of plant-fungal interactions across gradients requires a high level of
868 replication of small individual samples (< 0.2 mg root) within sites. As an effective
869 way to achieve this within limited budgets we used T-RFLP on individual roots (62).
870 At the time the samples were run it was not possible to achieve cost-effect next-
871 generation sequencing of highly replicated samples (n > 500), however we did pool
872 samples for next-generation sequencing (454-pyrosequencing) at the level of site (n
873 = 10). This comparison showed that the T-RFLP results captured similar patterns in
874 community composition and beta-diversity as next-generation sequencing (15), and
875 recent work suggests that these approaches can be as effective as deep sequencing
876 for detecting ecological patterns in microbial communities (63).
877
878 A subsample of 0.15 mg of each root was ground in a bead beater, then extracted
879 with Power Soil DNA Isolation Kit (Mo-Bio Labs, Carlsbad, CA, USA). Polymerase
880 chain reactions (PCRs) were carried out in a final volume of 20 µl, with 1µl of DNA
881 extract, 0.4µM of each primer, 0.2mM dNTP's, 2mM $MgCl_2$, 0.2 mg/ml BSA (New
882 England BioLabs, Ipswich, MA, USA) and 0.05U/µl Fast Taq DNA polymerase (Roche
883 Diagnostics N.Z., Ltd., Auckland, New Zealand). Thermal cycling for the PCRs started
884 with an initial denaturing step at 94°C for 3 min, followed by 35 cycles of 30 seconds
885 at 94°C, 1 min at 58°C and 1 min at 72°C, and ended with a final extension step of
886 72°C for 10 min. Five per cent of the PCRs did not amplify. For those samples, a
887 nested PCR was used combining a first PCR with NS1 and NS4 (universal fungal
888 primers (64)) as above, except that primer concentration was 0.1 µM and annealing
889 temperature 40°C, followed by NS31-VIC and AML2-6FAM. PCR products were
890 purified using DNA Clean & Concentrator Kit (Zymo Research Corporation, Irvine, CA,
891 USA).
892
893 T-RFLP restriction enzymes were chosen by running virtual digestions of 189
894 commercial restriction enzymes on the 10 most abundant sequences of a
895 pyrosequencing library generated from the pooled PCR products. Using virtual
896 digestions of 189 commercial restriction enzymes run on the 10 most abundant

897 arbuscular mycorrhizal sequences resulting from pyrosequencing, we selected the
898 enzymes HinfI (Life Technologies New Zealand Ltd., Auckland, New Zealand) and MslI
899 (New England BioLab) as having the greatest ability to distinguish molecular
900 Operational Taxonomic Units (OTUs). Clean PCR products were digested for 6 h and
901 1 h respectively and denatured using HiDi formamide mixed with MapMarker 1000
902 ROX standard (BioVentures, Murfreesboro TN, USA). Terminal restriction fragments
903 (TRFs) were separated by capillary electrophoresis using a Prism 3100 Genetic
904 Analyzer (Applied Biosystems) at the University of Canterbury Sequencing Centre
905 (Christchurch, New Zealand).
906
907 The TRAMPR package (62) for R (40) was used to process TRFLP data. Peaks with a
908 height ≤20% the height of the largest peak were ignored as background noise. The
909 *build.knowns* function from the TRAMPR package (with default settings) was used to
910 define TRFLP-OTUs by the highest peak from each restriction enzyme direction
911 (forward and reverse). TRFLP gave a total of 34 OTUs. For brevity, we henceforth
912 refer to fungal OTUs as "species".
913
914 *Plant amplification and sequencing*
915 Plant DNA from leaf and root samples was extracted using the Intron Plant DNA
916 extraction kit (Intron Biotechnology, Gyeonggi-Do, Korea) and amplified using the
917 chloroplast trnL (UAA) gene primers c and d (65). These primers failed to amplify
918 DNA from fern species, hence specific fern primers trnL- f and trn- Fern (66) were
919 used to amplify the DNA in the root samples for which PCR failed using trnL-c-d
920 primers. Amplicons from both leaf and root samples were purified using ExoI and
921 Sap enzyme (Thermo Fisher Scientific, Auckland New Zealand) and sequenced at the
922 University of Canterbury Sequencing Centre (Christchurch, New Zealand). Plant
923 species were identified based on BLAST matches to GenBank at 98% similarity,
924 including sequences from our vouchered plant leaf collections (GenBank KF591217 -
925 KF591315; KF591316 - KF591341).
926
927 *Justification of sequencing approach*

928 DNA-based methods not only provide an efficient means of data collection, but they
929 also allow the identification of cryptic taxa or those that are difficult to culture, and
930 are thus being increasingly used to document interactions among species for
931 network studies (67, 68). By sampling root tissue, we isolated fungi that were
932 symbiotic with the plant, but to be conservative we avoid assigning any direction to
933 the interactions, as they may be mutualistic, commensalistic or antagonistic,
934 depending on the taxa involved or their environmental context (68-70). This is
935 analogous to other network types where, for example, the visitation of flowers does
936 not necessarily imply successful pollination and fruit feeding does not imply
937 successful seed dispersal. We used the colonization of plant species by AMF species
938 at each site to generate community plant-AMF interaction networks, as in previous
939 studies (12, 36, 68).
940
941 *Controlling for the effect of species abundances in attachment and detachment*
942 *analyses*
943 Abundant species have a greater probability of being observed engaging in
944 interactions with others, which could make them more connected and/or central in
945 the interaction network. Likewise, if newly-arriving species interact with others at
946 random, they have a greater likelihood of interacting with abundant species by
947 chance. In this way, the abundance of species could drive both their network
948 position and probability of being attached to or detached from. Although the
949 processes of preferential attachment and detachment would still be useful to
950 understand, even if they were driven by abundances, we tested explicitly whether
951 centrality and degree affected attachment and detachment probability, after
952 controlling for differences in the abundance of species.
953
954 We first tested whether the abundance of species determined their network position
955 (centrality and/or degree), then we tested whether the preferential attachment
956 results changed after controlling for species abundances. To test these possibilities,
957 it is necessary to have an independent measure of species abundances from the site.
958 Defining and measuring the abundance of individual mycorrhizal fungal taxa in the
959 field presents numerous difficulties (71). Nevertheless, to account for their sampling

effort (rather than their 'abundance' as it would be perceived by a plant), we used their frequency in our samples (i.e. the number of plant root samples in which they were detected). However, plant abundances can be measured easily aboveground, and aboveground biomass/percentage cover has been shown to correlate with belowground biomass, which would be more important for belowground interactions.

All vascular plant species rooted within each plot were identified to species, and percentage cover measured using a relevé plot method. Briefly, cover was assessed visually as cover classes (<1%, 1–5%, 6–25%, 26–50%, 51–75%, 76–95% and >95%) within each of four height tiers (0–0.3 m, 0.3–2 m, 2–5 m, 5–12 m) following standard vegetation survey protocols (72). The midpoint for each cover class used to calculate percentage cover. We first tested whether the percentage cover of a plant species was a good predictor of its network centrality. We used a linear mixed effects model with closeness centrality as the response variable and percent cover as the predictor, with site age (chronosequence stage) as a random effect. We then ran an analogous model to test for an effect on plant degree. Because we did not have an independent measure of fungal abundance, we used their frequency in our samples (i.e. the number of plant root samples in which they were detected) as a surrogate for their abundance.

We first tested whether the percentage cover of a plant species was a good predictor of its network centrality. We used a linear mixed effects model with closeness centrality as the response variable and percent cover as the predictor, with site age (chronosequence stage) as a random effect. We then ran an analogous model to test for an effect on plant degree. We also re-ran our earlier models for preferential attachment including abundance of each species as a covariate.

Simulations of preferential attachment and detachment

Our finding that preferential attachment was explained better by centrality than by degree raises the question of how these differing non-random processes affect the final outcome of the network produced. The overall plant-AMF network architecture

992 was significantly nested (P = 0.009, measured using NODF), as observed in previous
993 plant-mycorrhizal networks (12). We therefore assessed the extent to which
994 (linear) preferential attachment and detachment, based on centrality vs. degree,
995 would affect the nestedness of networks. To do this, we conducted a set of
996 simulations of network assembly and disassembly scenarios. In each replicate of the
997 assembly process, we began with a network comprising four species (two plants and
998 two arbuscular mycorrhizal fungi, AMF), with three interactions among them. One
999 species of plant and one AMF each had two interactions, and the remaining two
1000 species had one interaction (this could be visualized as an upside-down 'L' in the
1001 adjacency matrix). Note that if we began with a smaller matrix (e.g. only one
1002 interaction between two species), a newly-arriving AMF species would have no
1003 option but to interact with the single plant species. Then a newly-arriving plant
1004 would choose between the two fungi with equal probability (they would have the
1005 same degree and centrality), and this would inevitably produce the matrix with
1006 which we began.
1007
1008 From this starting network, we simulated the arrival of new AMF and plant species
1009 (alternating between the trophic levels) through time, until the network contained
1010 50 plants and 50 fungi. At each time step, the newly-arriving species would interact
1011 with one existing species, with a probability proportional to the existing species'
1012 degree (i.e. the Barabasi and Albert model (4)) or closeness centrality. We also ran a
1013 third scenario whereby attachment was random (equally probable attachment to
1014 any existing species), to provide a null point of comparison. In the random
1015 attachment scenario, the lifetime probability of receiving new attachments (i.e.
1016 'fitness' in network, but not Darwinian terminology) was proportionate to the arrival
1017 order of species. Each newly-arriving species initially only interacted with one
1018 existing species, but it could also potentially interact with other species that arrived
1019 later.
1020
1021 After this assembly phase, each network was subjected to a disassembly phase,
1022 using the same scenario (degree-based, centrality-based or random) as was used
1023 during that network's assembly. Alternating plant and AMF species were removed

(i.e. went extinct) with a probability that was inversely proportional to the degree or closeness centrality of the species with which they interacted, such that species that interacted with species of high degree or high centrality were less likely to go extinct. If a species interacted with more than one other species, its detachment probability was determined by the mean degree or centrality of those species. If, after a species went extinct, other species were left unconnected (i.e. their only interaction partner went extinct), these unconnected species were also deemed to have gone secondarily extinct. As with the assembly phase, we ran a scenario of the disassembly phase whereby extinction was random. The simulated extinction of plant or AMF species proceeded until there remained only two species at that trophic level or until the network became too small to accurately calculate centrality. If only one trophic level met these criteria (e.g. if there remained only two plant species, but more than two AMF species), then the other trophic level continued to suffer extinctions until it also met the criteria (in Fig. S4, this results in primary extinctions that begin as multiples of two then eventually include single extinctions). Consequently, the number of primary extinctions during disassembly did not consistently increase by two during every time step, unlike the assembly phase, where two species attached in each time step.

Each scenario of the assembly and disassembly phases was run for 1000 replicates (each comprising multiple time steps). At each time step within each replicate, after species arrived or went extinct, we recorded the nestedness of the network. Nestedness is a network pattern whereby specialist species interact with a subset of the species that interact with generalists. It is a common feature of mutualistic networks (46), which has also been observed recently in plant-mycorrhizal networks (12) and has been shown to increase the persistence of networks (1, 2).

We calculated the nestedness of the network using NODF, calculated using the nestednodf function in the vegan package (45) for R. Because this measure could be influenced by network size, we scaled the observed NODF by the distribution of NODF values obtained by randomizing the adjacency matrix using the null model (“Null model II”) of Bascompte et al. (46). For each network at each time step, we

ran 99 iterations of the null model, each time calculating NODF. We subtracted the mean NODF value of the resulting null distribution from the observed NODF of the network, and divided the result by the standard deviation of the null distribution. This provided a standardized measure of the extent to which the nestedness of the network at each time step differed from null expectations for a network of that size.

SI Results

There was no change in network structure along the chronosequence

Previous work has shown that some attributes of network structure can be rapidly detected even with small samples from networks (37). This suggests that overall network architecture, such as interaction nestedness, could emerge quickly during ecosystem development (i.e. even when the network is small), provided that preferential attachment and detachment processes occur from the outset of network formation.

We therefore analyzed how nestedness and other metrics of network structure changed along the chronosequence using general linear models (or Poisson generalized linear models in the case of richness) with the metric as the response variable, and log site age as the predictor. As metrics to describe network structure, we tested two measures of nestedness (nestedness temperature and NODF), connectance, both quantitative and binary versions of linkage density, quantitative interaction evenness, and species richness of plants and mycorrhizas. To allow for the possibility that the relationship between network metrics and site age was non-linear, we included a quadratic term for site age. We also included sample size (the number of root samples where both the plant species and at least one fungal species were identified) as a covariate to account for any potential sampling biases. We then simplified each of these models by removing variables and minimizing the Akaike Information Criterion (AIC).

In our networks, nestedness did not change significantly across the chronosequence (Table S3), as would be expected if the strength of preferential attachment was consistent across the chronosequence. In fact, no measure of structure changed with ecosystem development (Table S3, Fig. S2), congruent with previous studies of the assembly of pollination network and food web structures (6, 73, 74). In contrast, a comparison of early and late successional forests found two (connectance and specialization) out of six measures of plant-AMF network structure changed (36), though these changes could have been caused by changes in the diversity of potential interaction partners. Despite the macroscopically static structure we

observed, there was high turnover of species and interactions, with new species joining the network and others no longer occurring at each stage along the sequence (Table S1).

Effect of species abundances on results

The effect of plant percent cover on centrality was significant ($t = 3.24$, $P = 0.002$), though the effect size was small (slope = 0.000217). For example, if a species' percent cover changed by 11% (which would be equivalent to changing from the lower quartile to the upper quartile), its fitted value for centrality would increase only by 0.002 (which is an order of magnitude less than one standard deviation for centrality, s.d. = 0.029). We note, however, that plant percent cover significantly predicted plant normalized degree ($t = 6.55$, $P = 2.46 \times 10^{-9}$), with a larger effect size (slope for the effect of percent cover on normalized degree = 0.010). The abundance of AMF taxa in samples significantly predicted their centrality (log transformed to make relationship linear: $t = 8.32$, $P < 0.0001$) and normalized degree ($t = 21.71$, $P < 0.0001$).

Thus, unsurprisingly, the network position of species was correlated with their abundance. However despite this, the influence of plant centrality on attachment and detachment probability of fungi remained significant (Table S4), even after controlling for species abundances (i.e. including abundance as a covariate to test whether centrality affected attachment or detachment probability at a given level of abundance). We used aboveground cover as a measure of plant abundance, which had the advantage of being measured independently from our plant-AMF associations. However, in case aboveground cover was not correlated with root abundance, we repeated the analyses with the abundance of each plant species in the root samples as a covariate, and the effect of plant centrality on fungal attachment remained significant (Table S4). In fact, plant abundance (using either measure) was not significantly correlated with AMF attachment probability (Table S4), though there was a non-significant tendency for AMF detachment probability to increase with plant abundance. In contrast to this consistent relation between

attachment or detachment and centrality, the relation between normalized degree and attachment or detachment probability of AMF became non-significant when abundance (either aboveground cover or abundance in samples) was included as a covariate ($|t| < 1$, $P > 0.343$ in both cases). This indicates that any of the variance in attachment or detachment probability that was attributable to normalized degree was also collinear with plant abundance, due to the strong correlation between abundance and degree.

Plants did not show any preferential attachment in the original analyses (Table S2), and the addition of abundance as a covariate did not alter this (Table S4). However, the formerly significant effect of AMF centrality on plant detachment probability became non-significant when the abundance of AMF taxa in samples was added as a covariate in the models. Moreover, the non-significant trend towards a positive correlation between AMF degree and plant detachment probability became significant when abundance was included in the model, in contrast with previous studies showing that species with high-degree are more likely to retain interactions and their partners have a reduced probability of extinction (7, 10).

1146 **SI Figure legends**

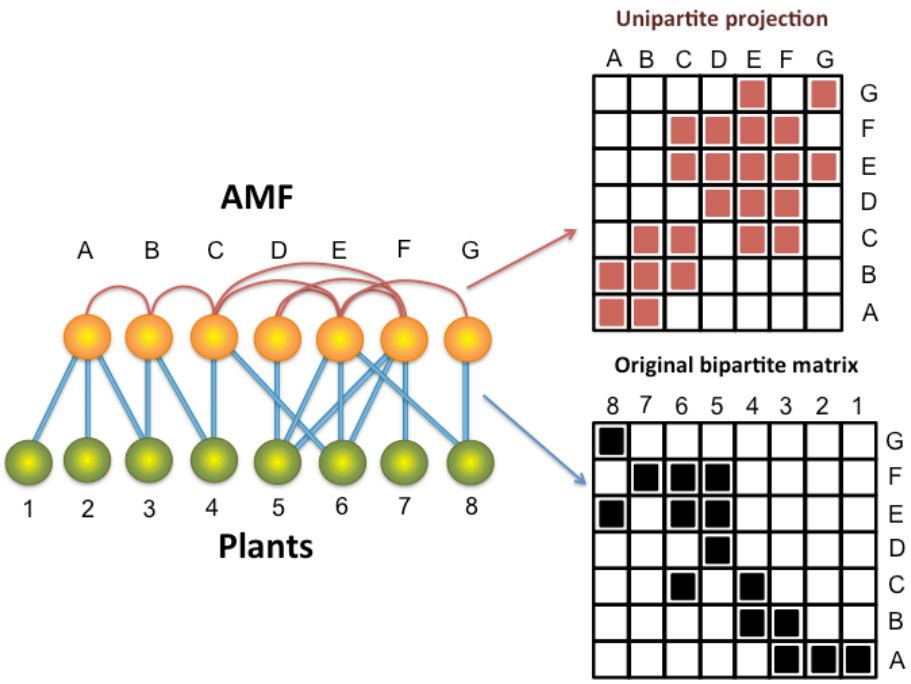

1147

1148 **Fig. S1 Measurement of partner overlap.** Illustration of a network of interactions
1149 among plants and arbuscular mycorrhizal fungi (AMF). The network can be depicted
1150 as a bipartite matrix, where black squares indicate the presence of an interaction
1151 ('link') in the network. A unipartite projection of this network can also be generated
1152 for each trophic level (here depicted in red, only for AMF), whereby species are
1153 linked when they share an interaction partner. This unipartite projection depicts
1154 interaction-partner overlap among species. We then measured each species' partner
1155 overlap as 'closeness centrality': the inverse of the mean path length (i.e. 'degrees of
1156 separation') from the focal species to all others in the unipartite projection. This
1157 distance has also been called 'functional specialization' (43). For example, species E
1158 is connected directly to species C, D, F and G, has two steps to species B (via C) and
1159 three steps to species A (via C and B). This gives species E a mean path length of 1.5
1160 to any other species, which is the shortest mean path length and the highest
1161 closeness centrality of any AMF species. Species A and G have the same number of
1162 links in the unipartite projection (1 link), but G shares a plant partner with species E
1163 that shares partners with many others in the network (mean path length of G = 2.3).
1164 In contrast, A shares a partner with species B, which itself only shares partners with
1165 A and C. Thus, A has a lower overall partner overlap (mean path length = 2.83)

because it does not share partners with plants in the largest cluster of interacting species.

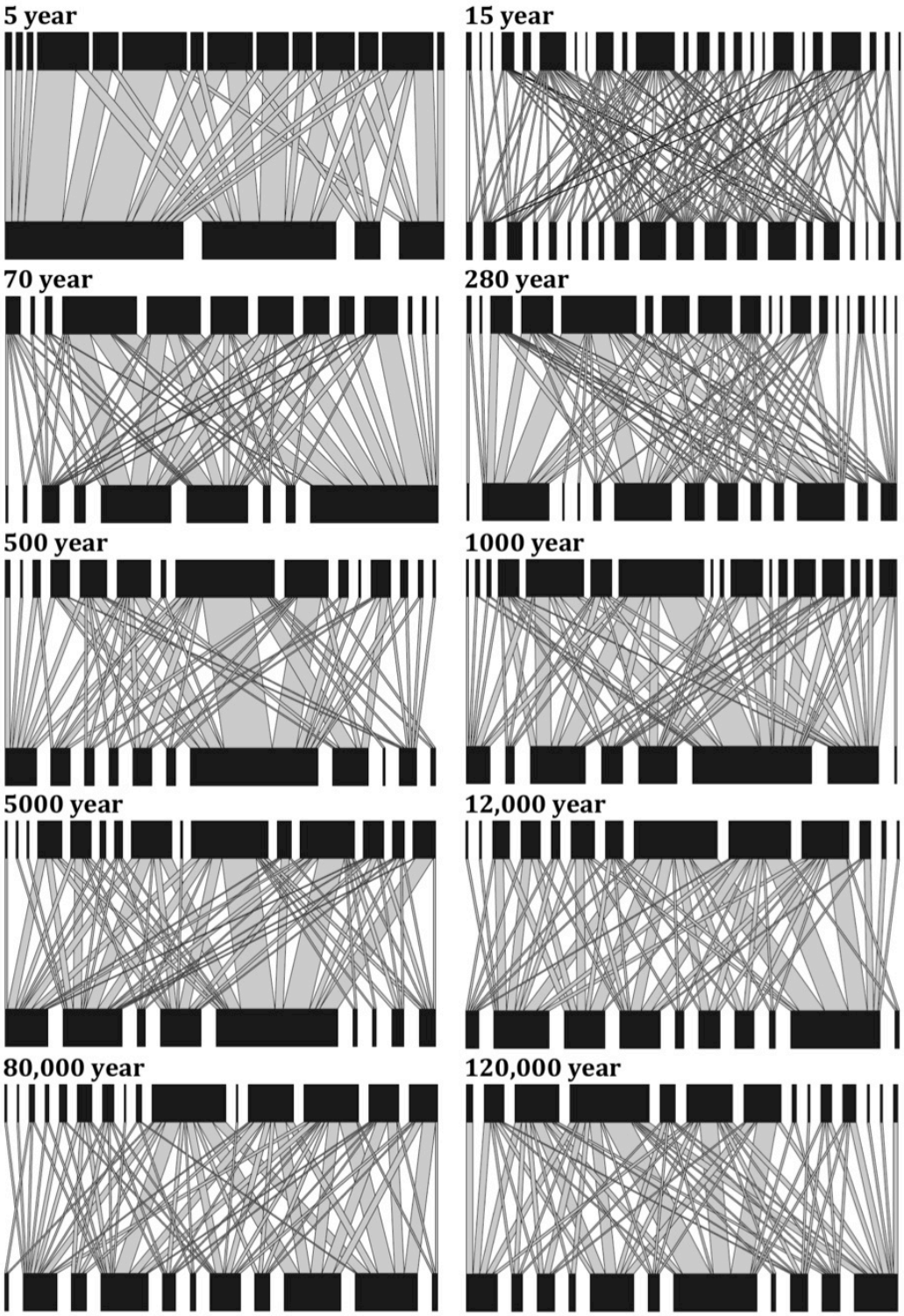

Fig. S2 Plant-AMF networks along chronosequence.

Quantitative networks are shown (whereby the width of links indicates their relative frequency). However, binary (links unweighted) networks were used for analysis because frequency of association is not an unbiased measure of interaction frequency in plant-mycorrhizal associations (69).

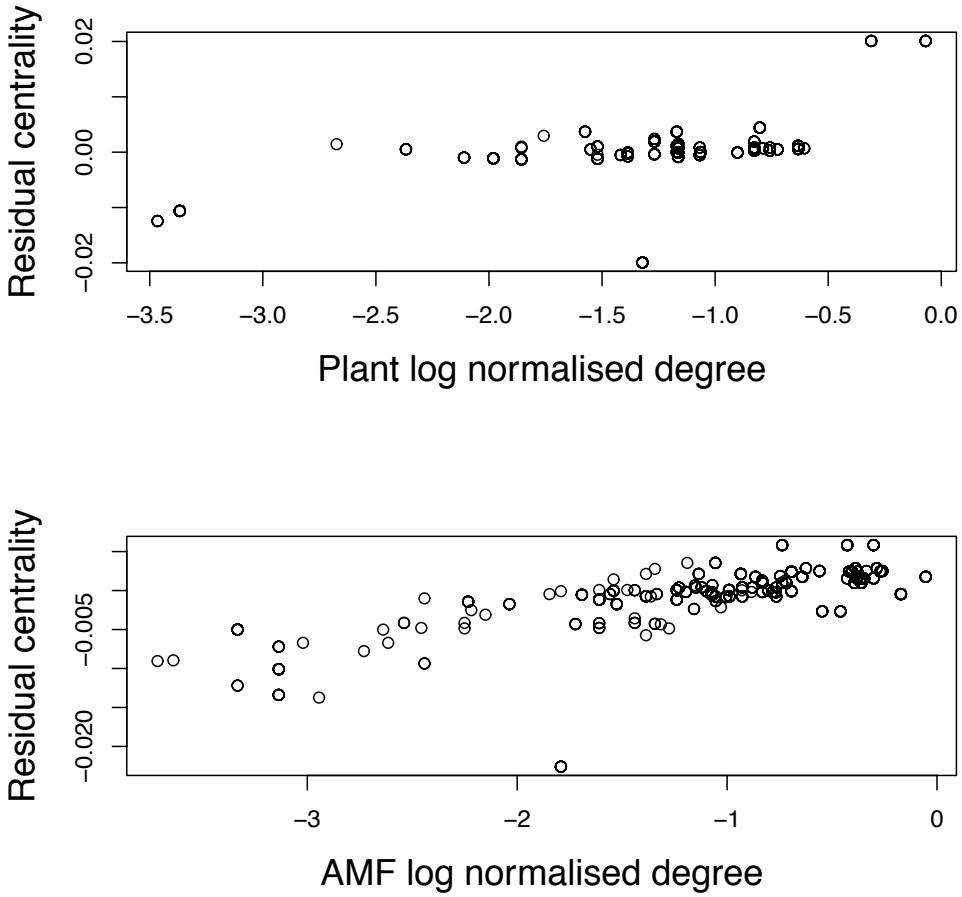

Fig. S3 Relationship between normalized degree and centrality. Because we compared preferential attachment based on interaction-partner overlap (defined as 'closeness centrality', Fig. S1) with a similar process based on degree, we tested whether degree and centrality were correlated. We conducted Gaussian mixed effects models with normalized degree (log transformed) as the predictor variable and closeness centrality as the response. To account for the non-independence of species from a given site, site age was included as a random effect. Mixed effects models were conducted in the 'lme4' package (39) for R. P values for the models were estimated using degrees of freedom calculated with the Satterthwaite method of denominator synthesis, carried out in the 'lmerTest' package (75) for R. In the figure, degree is log transformed and closeness centrality is presented as residuals after removing variation due to random effects. All relationships were significantly positive (mixed effects models: $t > 13$, $P < 0.0001$ in all cases).

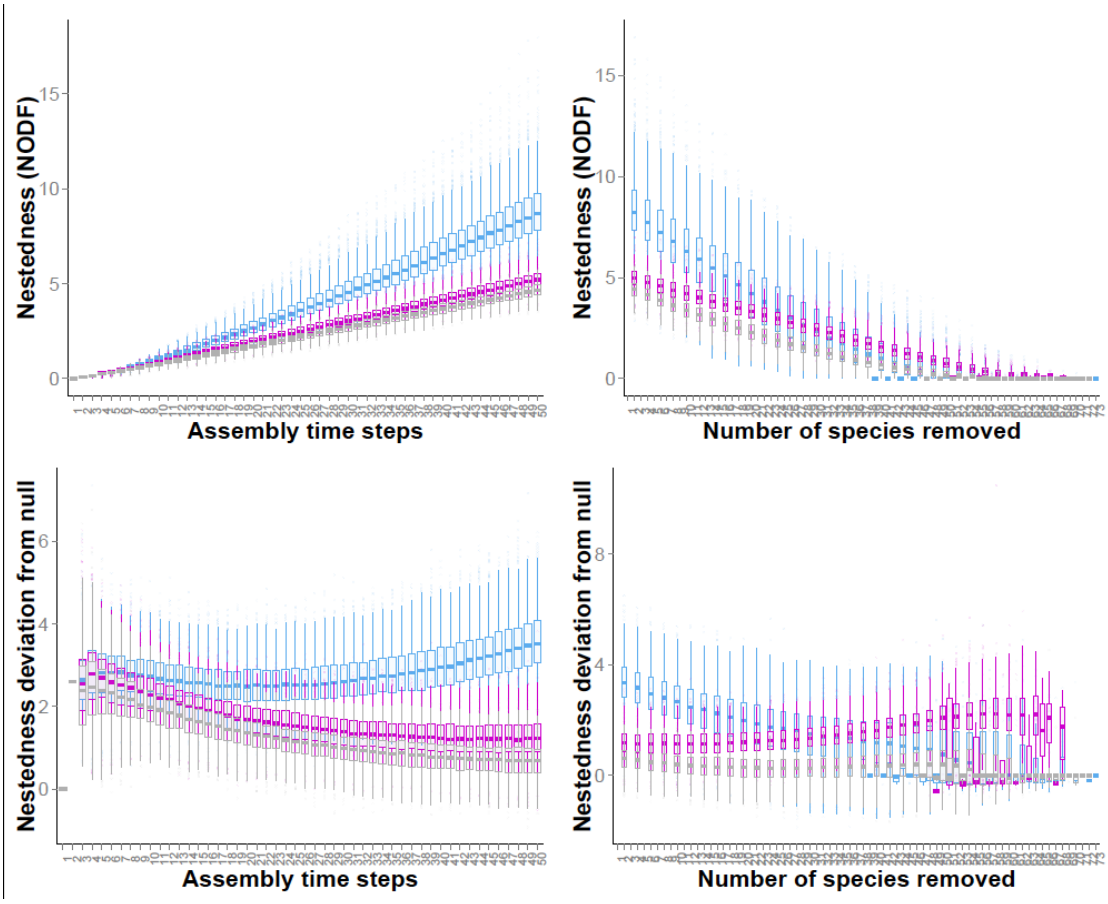

Fig. S4 Changes in interaction nestedness during simulated assembly and disassembly phases. Nestedness (raw NODF top row, deviation from null expectation bottom row) during simulated arrival (left column) and extinction (right column) of plant and AMF species. Each scenario was run for 1000 replicates. Dark horizontal lines show median values, boxes show upper and lower quartiles, and whiskers show minima and maxima (with points signaling extreme values). The scenarios were preferential attachment or detachment based on the degree (blue) or closeness centrality (purple) of interaction partners (or inverse of degree and centrality for detachment). For comparison, random extinctions are presented in grey. Both assembly and disassembly phases had notable impacts on network nestedness. During the assembly phase, the scenario based on preferential attachment to high-degree nodes produced networks that were highly nested, and considerably more nested than the other two scenarios. Nestedness tended to increase with network size (through time), emphasizing the need to compare raw nestedness against a null model. When compared against null expected nestedness, only the degree-based scenario had increasing nestedness through time. In contrast,

the centrality-based and random assembly scenarios showed a slight decrease in nestedness through time (as the addition of new nodes diluted the legacy of the starting matrix, which was highly nested). Despite this, the centrality-based scenario was consistently more nested than the random attachment scenario. Importantly, the differences between the degree- and centrality-based scenarios were reversed during the disassembly phase. As progressively more species were removed, the degree-based scenario showed a rapid decline in nestedness, whereas the centrality-based scenario became slightly more nested than null expectation (and more nested than the centrality-based scenario).

Table S1: Site details.

Details of site locations (Lat. = latitude, Long. = longitude), stage of ecosystem development, the number of plant and arbuscular mycorrhizal fungal (AMF) taxa sampled and interactions (Links) between them (with cumulative numbers up to, and including, that site in parentheses), and site conditions. Additional details can be found in Richardson et al. (30) and updated in Holdaway et al. (69).

Site age (years)	Stage	Lat.	Long.	Dominant vegetation	Plant taxa	AMF taxa	Links
<5	Progressive	-43.25	170.10	sparse herbfield	6	15	37
15	Progressive	-43.42	170.16	tall shrubland	20 (23)	24 (29)	113 (140)
70	Progressive	-43.42	170.16	early successional forest	9 (28)	13 (29)	57 (180)
290	Progressive	-43.41	170.18	broadleaved forest	13 (35)	19 (32)	73 (239)
500	Progressive	-43.41	170.17	broadleaved forest	11 (38)	15 (32)	55 (272)
1000	Progressive	-43.40	170.17	tall broadleaved forest	8 (41)	17 (32)	61 (307)
5000	Progressive	-43.40	170.17	tall broadleaved forest	9 (43)	15 (32)	61 (321)
12,000	Peak biomass	-43.33	170.21	tall broadleaved-podocarp forest	10 (46)	13 (32)	55 (344)
60,000	Retrogressive	-43.24	170.30	broadleaved-podocarp forest	11 (48)	15 (33)	64 (359)
120,000	Retrogressive	-43.25	170.19	short broadleaved-podocarp forest	11 (53)	14 (33)	61 (399)

Table S2: Coefficients tables from attachment and detachment models for plants and arbuscular mycorrhizal fungi (AMF). Coefficients tables for fixed effects component of generalised linear mixed models testing for correlation between attachment and detachment probability and (closeness) centrality (our measure of interaction-partner overlap, see Fig. S1) or degree. Response variables are binary (attached/detached vs. did not attach/detach), and a binomial error distribution with a logit link function was used. All models had site included as a random factor to control for the non-independence of any new associations occurring at the same point along the chronosequence. Separate models are presented for (normalized) degree vs. centrality, as described in the main text. Additional models are presented with both centrality and degree to demonstrate that the significance and direction of effect for centrality does not change (though that of degree does in some cases). For each response variable, the best-fitting model (lowest AIC) is in bold.

Response variable		**Estimate**	**Std. Error**	**Z**	**P**	**AIC**
AMF attachment probabilty	(Intercept)	-8.651	3.938	-2.197	0.028	60.2
	Degree	-1.112	1.325	-0.839	0.401	
	(Intercept)	-5.862	0.886	-6.616	< 0.0001	58.1
	Centrality	31.720	5.591	5.674	< 0.0001	
	(Intercept)	**-5.733**	**1.131**	**-5.067**	**< 0.0001**	**53.8**
	Centrality	**44.248**	**8.899**	**4.972**	**< 0.0001**	
	Degree	**-3.973**	**1.633**	**-2.433**	**0.015**	
Plant attachment probabilty	(Intercept)	-0.384	0.444	-0.864	0.388	522.3
	Degree	-0.112	0.534	-0.209	0.835	
	(Intercept)	**-1.065**	**0.865**	**-1.231**	**0.218**	**522.0**
	Centrality	**15.972**	**19.968**	**0.800**	**0.424**	
	(Intercept)	-1.747	0.975	-1.793	0.073	523.1
	Centrality	40.984	27.932	1.467	0.142	
	Degree	-0.734	0.700	-1.048	0.295	
AMF detachment probabilty	(Intercept)	-3.259	1.256	-2.595	0.009	421.9
	Degree	1.820	0.885	2.057	0.040	
	(Intercept)	1.084	0.537	2.019	0.044	417.7
	Centrality	-95.425	22.235	-4.292	< 0.0001	
	(Intercept)	**0.834**	**0.632**	**1.320**	**0.187**	**411.4**
	Centrality	**-121.885**	**28.563**	**-4.267**	**< 0.0001**	
	Degree	**2.646**	**0.934**	**2.835**	**0.005**	
Plant detachment probabilty	(Intercept)	-0.256	0.589	-0.435	0.664	602.5
	Degree	0.247	0.442	0.558	0.577	
	(Intercept)	2.252	0.327	6.890	< 0.0001	593.8
	Centrality	-48.616	7.554	-6.436	< 0.0001	
	(Intercept)	**2.149**	**0.329**	**6.527**	**< 0.0001**	**593.2**
	Centrality	**-54.633**	**8.486**	**-6.438**	**< 0.0001**	
	Degree	**0.759**	**0.476**	**1.594**	**0.111**	

Table S3: No significant change in network architecture along the chronosequence. Results of best-fitting models for each metric of plant-mycorrhizal network structure (response variable) and any predictor variables that were retained after model simplification. The maximal model contained sample size (number of samples yielding an identifiable sequence) and site age and a quadratic site age term (to allow for nonlinear relationships) as predictors. We compared all subsets of this maximal model and selected the best-fitting model with the lowest AIC score. Raw P values are provided, though these are non-conservative because multiple testing increases the probability of Type I error. Where no predictors are given, the best-fitting model contained only an intercept. No measure of network structure changed significantly along the chronosequence.

Response	**Predictor**	**D.F.**	**F**	**P**
Nestedness (NODF)	Sample size	1,8	4.3	0.073
Nestedness temperature	Sample size	1,8	1.9	0.207
Connectance	< none >			
Binary linkage density	< none >			
Weighted linkage density	Sample size	1,6	1.7	0.234
	Log site age	1,6	0.0	0.931
	(Log site age)^2	1,6	1.6	0.253
Interaction evenness	Sample size	1,8	4.1	0.077
Plant richness	< none >			
Mycorrhizal richness	Sample size	1,6	3.4	0.113
	Log site age	1,6	0.2	0.697
	(Log site age)^2	1,6	3.0	0.133

Table S4: Coefficients tables for preferential attachment and detachment models with centrality as predictor, controlling for abundance. Coefficients tables for fixed effects component of generalized linear mixed models testing for correlation between attachment and detachment probability and closeness centrality, our measure of interaction-partner overlap (see Fig. S1). This table is analogous to Table S2), but with the abundance of species included as a covariate. The abundance refers to that of the interaction partner (not the species attaching), and is measured using the aboveground percent cover for plants and the abundance in samples (number of roots in which it occurred) for the fungi. For completeness, we also present models with plant abundance measured using the number of samples in which it occurred (as with fungi).

Response variable		**Coefficient**	**Std. Error**	**Z**	**P**
AMF attachment probability	(Intercept)	-5.925	1.366	-4.339	< 0.0001
	Percent cover	0.004	0.063	0.062	0.951
	Centrality	32.057	7.879	4.069	< 0.0001
	(Intercept)	-5.681	1.370	-4.147	< 0.0001
	Sample abundance	-0.020	0.119	-0.165	0.869
	Centrality	31.016	6.862	4.52	< 0.0001
Plant attachment probability	(Intercept)	-1.092	1.181	-0.925	0.355
	Sample abundance	-0.001	0.010	-0.067	0.946
	Centrality	16.921	30.149	0.561	0.575
AMF detachment probability	(Intercept)	0.305	0.254	1.203	0.229
	Percent cover	0.011	0.006	1.813	0.070
	Centrality	-72.357	9.615	-7.525	< 0.0001
	(Intercept)	0.275	0.267	1.028	0.304
	Sample abundance	0.024	0.014	1.772	0.076
	Centrality	-72.342	10.088	-7.171	< 0.0001
Plant detachment probability	(Intercept)	0.196	1.110	0.176	0.860
	Sample abundance	0.008	0.003	2.368	0.018
	Centrality	-9.550	21.276	-0.449	0.654